Virologica Sinica (2021) 36:476–489
https://doi.org/10.1007/s12250-020-00316-0

www.virosin.org
www.springer.com/12250

RESEARCH ARTICLE

Generation of A Stable GFP-reporter Zika Virus System for High-throughput Screening of Zika Virus Inhibitors

Jing-Wei Zhang[1] · Han Wang[1] · Jing Liu[1] · Le Ma[1] · Rong-Hong Hua[1] · Zhi-Gao Bu[1,2]

Received: 31 July 2020 / Accepted: 18 September 2020 / Published online: 24 November 2020
© Wuhan Institute of Virology, CAS 2020

Abstract

Zika virus (ZIKV) is associated with severe birth defects and Guillain-Barré syndrome and no approved vaccines or specific therapies to combat ZIKV infection are currently available. To accelerate anti-ZIKV therapeutics research, we developed a stable ZIKV GFP-reporter virus system with considerably improved GFP visibility and stability. In this system a BHK-21 cell line expressing DC-SIGNR was established to facilitate the proliferation of GFP-reporter ZIKV. Using this reporter virus system, we established a high-throughput screening assay and screened a selected plant-sourced compounds library for their ability to block ZIKV infection. More than 31 out of 974 tested compounds effectively decreased ZIKV reporter infection. Four selected compounds, homoharringtonine (HHT), bruceine D (BD), dihydroartemisinin (DHA) and digitonin (DGT), were further validated to inhibit wild-type ZIKV infection in cells of BHK-21 and human cell line A549. The FDA-approved chronic myeloid leukemia treatment drug HHT and BD were identified as broad-spectrum flavivirus inhibitors. DHA, another FDA-approved antimalarial drug effectively inhibited ZIKV infection in BHK-21 cells. HHT, BD and DHA inhibited ZIKV infection at a post-entry stage. Digitonin was found to have inhibitory activity in the early stage of viral infection. Our research provides an efficient high-throughput screening assay for ZIKV inhibitors. The active compounds identified in this study represent potential therapies for the treatment of ZIKV infection.

Keywords Zika virus (ZIKV) · GFP reporter virus · High-throughput screening · Antiviral drug discovery

Introduction

Although Zika virus (ZIKV) was discovered 70 years ago (Dick *et al*. 1952), the virus has not caused a large-scale outbreak or serious infections and has therefore received little attention. The massive ZIKV outbreak in Brazil in 2015 linked ZIKV infections with severe neurological complications such as Guillain-Barré syndrome (GBS) in adults and congenital malformations in the fetuses of women infected with ZIKV during pregnancy (Petersen *et al*. 2016; França *et al*. 2016). Because of this, ZIKV caused a public health emergency of international concern (Gulland 2016; Chitti *et al*. 2016) and attracted universal attention.

To date, no specific treatment or licensed vaccine for ZIKV infection is available. So specific antiviral therapies and vaccines are urgently required. Virus reverse-genetic systems are powerful tools for the development of therapies and vaccines against ZIKV. Due to the instability of the cloned flavivirus genome (Pu *et al*. 2011; Zheng *et al*. 2016; Münster *et al*. 2018), it is difficult to construct a plasmid containing a full-length genomic infectious flavivirus clone; however, scientists have successfully rescued recombinant ZIKV viruses using different reverse-genetic systems and strategies. These include the transfection of *in vitro*-transcribed genomic RNA derived from

Electronic supplementary material The online version of this article (https://doi.org/10.1007/s12250-020-00316-0) contains supplementary material, which is available to authorized users.

✉ Zhi-Gao Bu
buzhigao@caas.cn

✉ Rong-Hong Hua
huaronghong@163.com

[1] State Key Laboratory of Veterinary Biotechnology, Harbin Veterinary Research Institute of Chinese Academy of Agricultural Sciences, Harbin 150069, China

[2] Jiangsu Co-Innovation Centre for Prevention and Control of Important Animal Infectious Disease and Zoonoses, Yangzhou University, Yangzhou 225009, China

plasmids containing the T7 promoter (Shan *et al*. 2016; Yang *et al*. 2017; Münster *et al*. 2018), direct transfection with plasmids containing DNA and the CMV promoter (Tsetsarkin *et al*. 2016; Schwarz *et al*. 2016), multi-fragment *in vitro* ligation transcription from the T7 promoter (Weger-Lucarelli *et al*. 2017; Widman *et al*. 2017; Deng *et al*. 2017), and multi-fragment transcription in cell recombination from the CMV promoter (Gadea *et al*. 2016; Atieh *et al*. 2016; Kobayashi *et al*. 2017). In these reverse-genetic system platforms, reporter viruses are generated that either expressed *Renilla* luciferase (Rluc) (Shan *et al*. 2016; Münster *et al*. 2018), turbo far-red fluorescent protein FP635 (Münster *et al*. 2018) or GFP (Gadea *et al*. 2016). However, reporter Zika viruses are unstable after a limited number of passages on normal susceptible cells. Gadea *et al*. (2016) reported that recombinant ZIKV virus that expressed *GFP* lost the *eGFP* gene from the third passage on Vero cells. Reporter Zika virus expressing the *RLuc* gene was also unstable when passaged on Huh7 cells and Rluc activity steadily decreased with each passage and was lost after passage three (Münster *et al*. 2018). Moreover, reporter-gene insertion attenuated the replication efficiency of recombinant virus in normal susceptible cells, resulted in a low virus titer and the absence of plaques (Shan *et al*. 2016; Münster *et al*. 2018). Therefore, for studies involving live-cell imaging microscopy and/or high-throughput screening assays, more stable and more efficient reporter Zika virus systems are urgently required.

This study reports the development of a ZIKV reverse-genetic system using homologous recombination methods. A stable ZIKV GFP-reporter virus system with considerably improved GFP visibility was developed, based on the genome sequence of Brazil epidemic strain ZIKV (Paraiba_01/2015). Using this reporter virus system, we established a high-throughput screening assay and screened a selected plant-sourced compounds library (TargetMol, Catalog No. L4600) for their ability to block ZIKV infection. Four compounds were identified that effectively inhibited ZIKV infection in cells. Two of these compounds are FDA-approved drugs, and here we report the anti-flaviviral activity of these two drugs for the first time. The active compounds identified in this study represent potential therapies for the treatment of ZIKV infection.

Materials and Methods

Cells, Viruses, and Antibodies

Human Embryo Kidney (HEK)-293T cells (ATCC, CRL-3216), Vero cells (ATCC, CCL-81), and BHK-21 cells (ATCC, CCL-10) were grown in Dulbecco's modified Eagle's medium (DMEM; Gibco C11995500CP) supplemented with 10% heat-inactivated fetal bovine serum (FBS; Gibco, 10099-141), 100 U/mL penicillin and 100 μg/mL streptomycin, at 37 °C in 5% CO_2. For HEK-293 T cell cultures, cell culture plates were covered with poly-D-lysine hydrobromide (Sigma P7886) at 50 μg/mL. The BHK-DR cell line (generated from BHK-21 cells as parental cells in this study), which stably expresses the dendritic cell-specific ICAM-3 grabbing non-integrin related protein (DC-SIGNR) that as a cell receptor may enhance the efficiency of virus infection, was maintained in DMEM supplemented with 10% FBS, 100 U/mL penicillin, 100 μg/mL streptomycin and 1 mg/mL G418 at 37 °C in 5% CO_2. Zika virus and reporter Zika virus generated in this study were propagated on Vero cells and BHK-DR cells, respectively, and were titrated on BHK-21 cells and BHK-DR cells, respectively. Rabbit polyclonal antibodies against Zika virus envelope protein were obtained from GeneTex (GTX133314). Alexa Fluor 680-conjugated donkey anti-mouse IgG antibodies were obtained from Thermofisher Scientific (A10038). IRDye 800CW-conjugated donkey anti-rabbit IgG antibodies were obtained from LI-COR (926-32213). Chloroquine (Sigma C6628) and 6-azauridine (Sigma A1882) were obtained from Sigma.

Plasmid Construction

To rescue Zika virus via homologous recombination in mammalian cells, the Paraiba_01/2015 strain of ZIKV, a Brazil 2015 epidemic strain was chosen as the sequence reference (GenBank accession number: KX280026). The Paraiba_01/2015 strain of ZIKV was isolated in the state of Paraiba (Brazil) in 2015 from serum of a febrile female (Tsetsarkin *et al*. 2016). The DNA-based ZIKV subgenomic replicon plasmid pZIKVrepdCME was constructed using the strategy described previously (Li *et al*. 2017b). The fragment of the first quarter of the ZIKV genome containing 5′-UTR-C-prM-E-$NS1_{134}$ was synthesized and cloned into vector pCAGneo (Hua *et al*. 2014b) via *Xho*I and *Not*I restriction sites and the sequence-verified constructs were named pZCME-$NS1_{134}$. To generate a GFP-expressing reporter virus, the GFP-encoding sequence fused to sequences encoding the first 33 amino acids of the C protein and the FMDV 2A coding sequence were inserted into pZCME-$NS1_{134}$ between the 5′-UTR and the C protein gene. This construct was named pZC38GFP-CME-$NS1_{134}$.

The pCAG-DC-SIGNR construct expressing DC-SIGNR was constructed by cloning the synthesized DC-SIGNR-coding sequence (GenBank accession number: AY042234) into the *Sac*I and *Xho*I restriction sites of pCAGneo.

DNA Transfection and Virus Production

To generate recombinant virus, the DNA fragments containing the CMV promoter and coding sequence for structural proteins were amplified by PCR from plasmids pZCME-NS1$_{134}$ or pZC38GFP-CME-NS1$_{134}$. For both plasmids, the PCR primers were: 5′-GGCCTTTTGCTCACATGGCTCGACAG-3′ and 5′-GACTGCTGCTGCCAATCTACGGGGG-3′. The replicon plasmid pZIKVrepdCME was linearized using *Xho*I. The PCR products and linearized plasmids were purified using a DNA purification Kit (Omega, D2500-01). HEK-293T cells (90% confluent), were transfected with linearized plasmid and PCR-amplified DNA fragments using Lipofectamine LTX and PLUS Reagent (Invitrogen 15338-100). Three days following transfection, the supernatants were inoculated onto Vero and BHK-21 cells and the virus-infected cell cultures were harvested after 3 to 4 days. After three freezing-thaw cycles, the cell cultures were stored at − 80 °C for analysis.

Establishment of DC-SIGNR-Expressing Stable Cell Lines

The BHK-DR cell line stably expressing the DC-SIGNR protein was generated by transfection of BHK-21 cells with plasmid pCAG-DC-SIGNR as described previously (Hua *et al*. 2014a, b). Briefly, a monolayer of BHK-21 cells was transfected with the pCAG-DC-SIGNR plasmid using Lipofectamine LTX and PLUS Reagent (Invitrogen 15338-100). Two days later, transfected cells were digested and cloned by limited dilution in 96-well plates and grew in medium containing G418. The cloned cells were selected by indirect immunofluorescence assay (IFA) with mouse monoclonal antibody against DC-SIGN1/DC-SIGN2 (Sigma, D2691). The selected clone was designated BHK-DR and maintained in G418-supplemented medium for further characterization and inoculation of ZIKV-GFP in high-throughput screening.

Immunofluorescence Assay (IFA)

Virus-infected cells or BHK-DR cells were fixed with 4% paraformaldehyde for 20 min at room temperature, permeabilized with 0.1% Triton X-100 in phosphate-buffered saline (PBS) at 4 °C for 10 min, and incubated with 4% bovine serum albumin V in PBS at 37 °C for 30 min. ZIKV was stained with pan-flavivirus E protein-specific mouse MAb 4G2 at 37 °C for 1 h or 4 °C overnight, then incubated with Fluorescein-Conjugated AffiniPure Goat Anti-Mouse IgG (ZSGB-BIO, ZF-0312) and Hoechst 33342 (Thermo 62249). To detect the expression of DC-SIGNR, the primary antibody was a mouse monoclonal antibody against DC-SIGN1/DC-SIGN2 (Sigma, D2691). After three washes with PBS, cells were visualized using a fluorescence microscope (Life, EVOSFL).

Plaque-forming Unit Assay

Approximately 2×10^5 cells/well BHK-21 cells (for rcZIKV) or BHK-DCR cells (for rcZIKV-GFP) in 0.5 mL DMEM medium supplemented with 5% heat-inactivated FBS were seeded in 24-well plates, and 24 h later, the monolayers were inoculated with 100 μL of serially diluted virus. The viruses were diluted with DMEM medium without FBS. After 6 h, 0.6 mL 3% methyl cellulose (Sigma M6385) was added to each well. At 6 days after infection, supernatants were discarded and cells were stained with 1 mL crystal violet-formaldehyde stain for 15–20 min. Plates were washed twice with water and were air-dried. The resulting plaques were counted and plaque-forming units per mL were calculated.

SDS-PAGE and Western blotting

Protein samples were separated by 12.5% SDS-PAGE, transferred onto a polyvinylidene difluoride (PVDF) membrane. To visualize proteins by immunoblotting, the following were used as primary antibodies: rabbit polyclonal antibodies against ZIKV E protein (GeneTex, GTX133314), mouse monoclonal antibody against GAPDH (Proteintech, 60004-1-Ig), rabbit polyclonal antibodies against GAPDH (Proteintech, 10494-1-AP). Primary antibodies were detected using Alexa Fluor 680 Donkey Anti-Mouse IgG secondary antibodies (Thermofisher Scientific, A10038) or IRDye 800CW Donkey Anti-Rabbit IgG (LI-COR 926-32213). Following four washes with PBS, signal detection was performed using a near-infrared fluorescence scanning imaging system (Licor Odyssey).

Antiviral Screening Assay

Approximately 3×10^4 cells/well BHK-DR cells in 100 μL DMEM medium supplemented with 5% heat-inactivated FBS were seeded onto CellCarrier-96 microplates (catalog number 6005550; PerkinElmer). After incubating the cells at 37 °C for 16 h, 50 μL dilutions of compounds were added to the cells. Approximately 1 h after addition of the compounds, 50 μL ZIKV-GFP was added to each well. Three wells of mock-infected cells and three wells of ZIKV-GFP-infected vehicle-treated cells were used on each plate as controls. The infected cells were incubated for 48 h at 37 °C. Cell nuclei were stained with Hoechst 33342 (Thermo 62249). Infected cells were visualized

using a high-content-screening microplate imaging reader (Operetta; PerkinElmer). Fifty-nine fields per well were imaged using a 20× objective. The images were analyzed using Acapella high-content imaging and analysis software. The infection-positive cell rates and total cell counts were all normalized to those of vehicle-treated control wells.

High-throughput Screening of A Selected Plant-sourced Compound Library

A library of 974 selected plant-sourced compounds was purchased from TargetMol (L4600). The compounds were stored as 10 mmol/L stock solutions in DMSO at − 80 °C until use. The first round of high-throughput screening was performed at a concentration of 10 μmol/L for each compound in triplicate. The criteria used to identify the primary candidates were a mean level of inhibition of ≥ 80% and relative cell viability of ≥ 90%.

Compound Validation Studies

Compounds selected in the primary screens were further evaluated by the same protocol as the primary screen, except that the compounds were serially diluted to final concentrations of 100 μmol/L, 10 μmol/L, 4 μmol/L, 2 μmol/L, 1 μmol/L, 0.5 μmol/L, 0.25 μmol/L, and 0.1 μmol/L. The 50% inhibition concentration (IC_{50}) and 50% cytotoxicity concentration (CC_{50}) were estimated using a nonlinear regression model from GraphPad Prism 5 software. The ability of four compounds with an IC_{50} < 1 μmol/L to inhibit viral replication was further evaluated in BHK-21 and A549 cells with wild-type recombinant ZIKV. One-hour following treatment with compounds at concentration of 8 μmol/L, 4 μmol/L, 2 μmol/L, 1 μmol/L, 0.5 μmol/L and 0 μmol/L, cells were infected with ZIKV at an MOI of 0.01. At 48 hpi, The ZIKV E protein expression level was determined and the amount of virus in the supernatant was titered to evaluate the inhibition efficiency of the compounds.

Time-of-addition Experiment

To evaluate which stage of the ZIKV life cycle was inhibited by each treatment, a time-of-addition experiment was performed as previously described (Chen *et al*. 2017; Aoki-Utsubo *et al*. 2018). Briefly, BHK-21 cells were infected ZIKV for 1 h (0 to 1 h). The test compounds were incubated with the cells or virus for 1 h before infection (− 1 to 0 h), during infection (0 to 1 h), and post-infection (1 to 48 h). At 48 h post infection, the supernatants were titrated and the cell lysates were immunoblotted to detect the viral protein expression level.

Statistical Analysis

All statistical analyses were accomplished using GraphPad Prism 5. The *P* value was calculated using an unpaired Student's *t*-test. $P > 0.05$ was considered non-statistically significant (n.s.), and $P < 0.05$ was considered statistically significant, marked as follows: *, $P < 0.05$; **, $P < 0.01$; ***, $P < 0.001$.

Results

Generation of Recombinant Zika Virus via Homologous Recombination

To produce recombinant ZIKV, we first constructed a DNA-based replicon system pZIKVrepdCME (Fig. 1A). The first quarter of the ZIKV genome, containing 5′-UTR-C-prM-E-$NS1_{134}$, was synthesized and cloned into the pCAGneo vector under transcriptional control of the CMV promoter and resulted in pZCME-$NS1_{134}$. To generate the GFP-expressing ZIKV reporter, plasmid pC38GFP-CME-$NS1_{134}$ was derived from pZCME-$NS1_{134}$, in which the *GFP* reporter gene followed by the sequence encoding FMDV 2A was cloned in-frame downstream of sequences encoding the additional first 38 amino acids of the C protein and upstream of the complete C protein (Fig. 1A). The 2A protease ensured the authentic N-terminus of the C protein. DNA fragment A, containing the CMV promoter and 5′-UTR-C-prM-E-$NS1_{134}$ of ZIKV, was amplified by PCR and was then used, in addition to linearized replicon plasmids, to transfect 293T cells (Fig. 1B). And DNA fragment B, which contained sequences of the CMV promoter and 5′-UTR-C38-GFP-2A-C-prM-E-$NS1_{134}$, was amplified by PCR. Cells of 293T were transfected with linearized replicon plasmids and fragment B (Fig. 1B).

At 3 days post transfection, the supernatants were inoculated onto BHK-21 cells and infectious viruses were detected using an immunofluorescence assay (IFA) with pan-flavivirus E protein-specific mouse MAb 4G2 (Fig. 2A). The recombinant ZIKV was cytopathic and formed plaques in BHK-21 cells (Fig. 2B) and Vero cells (data not shown). Recombinant ZIKV grown on BHK-21 cells reached an infectious titer up to 5.7 log PFU/mL at 72 h post-infection (hpi) and then the virus titer decreased at 96 hpi and 120 hpi. Viral growth dynamics were then analyzed on Vero cells and the virus titer reached 6.7 log PFU/mL at 48 hpi and was maintained at 7.0 log PFU/mL from 72 to 120 hpi (Fig. 2C). These results showed that the replication of recombinant ZIKV in Vero cells was highly efficient. For rescuing ZIKV-GFP, at 3 days post transfection, the supernatants were inoculated onto BHK-21 and

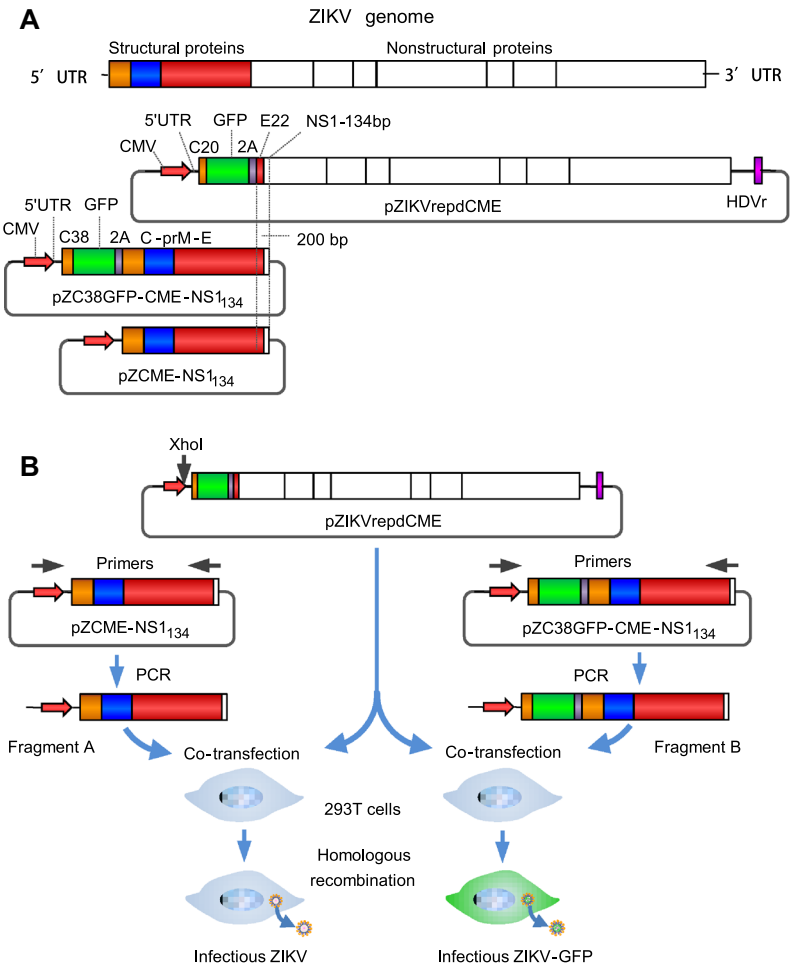

Fig. 1 Schematic representation of the strategy for plasmid construction and the production of recombinant ZIKV and ZIKV-GFP. **A** Illustration of the ZIKV genome and constructs used in this study. In the pZIKVrepdCME construct, the GFP- and FMDV-2A-coding sequences were inserted downstream of sequences encoding the first 20 amino acids of the C gene and upstream of sequences encoding the last 22 amino acids of the E gene. The 3′ untranslated region was flanked with HDVr to ensure the authenticity of the 3′ terminus of the transcribed RNA. **B** Schematic diagrams for the production of recombinant ZIKV and ZIKV-GFP marker viruses. DNA fragments containing the CMV promoter and the coding sequences of structural proteins were amplified by PCR. The purified PCR products and enzyme-linearized ZIKV replicon plasmid DNA were pooled and transfected into HEK-293T cells to generate infectious ZIKVs.

Vero cells to detect the titer of infectious virus. Positive GFP-expressing BHK-21 cells (Fig. 2D) and Vero cells were observed following inoculation with supernatants of transfected 293T cells. The infection of Vero cells with the recombinant reporter virus ZIKV-GFP caused cytopathic effects and led to plaque foramtion (data not shown). The infectious titer of ZIKV-GFP grown in Vero cells reached 6.5 log $TCID_{50}$/mL at 72 hpi (Fig. 2E). However, the GFP signal in infected Vero cells was mainly observed as distinct foci of green fluorescence signal, which did not conform to the shape of cells (Fig. 2F). This observation weakens the utility of of ZIKV-GFP as a reporter virus. In infected BHK-21 cells, the green fluorescence signal was evenly distributed throughout the cytoplasm and the cell outline was apparent (Fig. 2D and 2F). However, the replication of ZIKV-GFP in BHK-21 cells was attenuated compared with that of wild-type recombinant ZIKV growth in BHK-21 cells. In BHK-21 cells infected with ZIKV-GFP, the green fluorescence foci spread very slowly (Supplementary Fig. S1) and ZIKV-GFP did not cause cytopathic effects in BHK-21 cells even after incubation for 6 dpi or longer (Fig. 2D).

Generation of A Stable DC-SIGNR-expressing Cell Line BHK-DR for the Propagation of Recombinant ZIKV-GFP Reporter Virus

DC-SIGNR as receptor of flavivirus could increase the susceptibility of cells to ZIKV infection. To make ZIKV-GFP a more readable and stable genetic reporting tool for viral replication studies and inhibitor screening, we decided to establish a cell line that stably expressed DC-SIGNR, to enhance the replication efficiency of ZIKV-GFP. Following transfection, selection with G418 and IFA identification, one clone was selected to further evaluate its ability to enhance the replication of ZIKV-GFP and was named BHK-DR. DC-SIGNR was expressed on cell membranes and in the cytoplasm (Supplementary Fig. S1). As expected, ZIKV-GFP replicated and the foci of GFP fluorescence spread more efficiently in BHK-DR cells than in BHK-21 cells (Supplementary Fig. S1). Infection with ZIKV-GFP caused cytopathic effects (Fig. 2D) and formed plaques (Fig. 2B) in BHK-DR cells. The virus titer reached a plateau at 6.5 log $TCID_{50}$/mL at 72 hpi. The growth kinetic of ZIKV-GFP in BHK-DR cells was similar to that in Vero

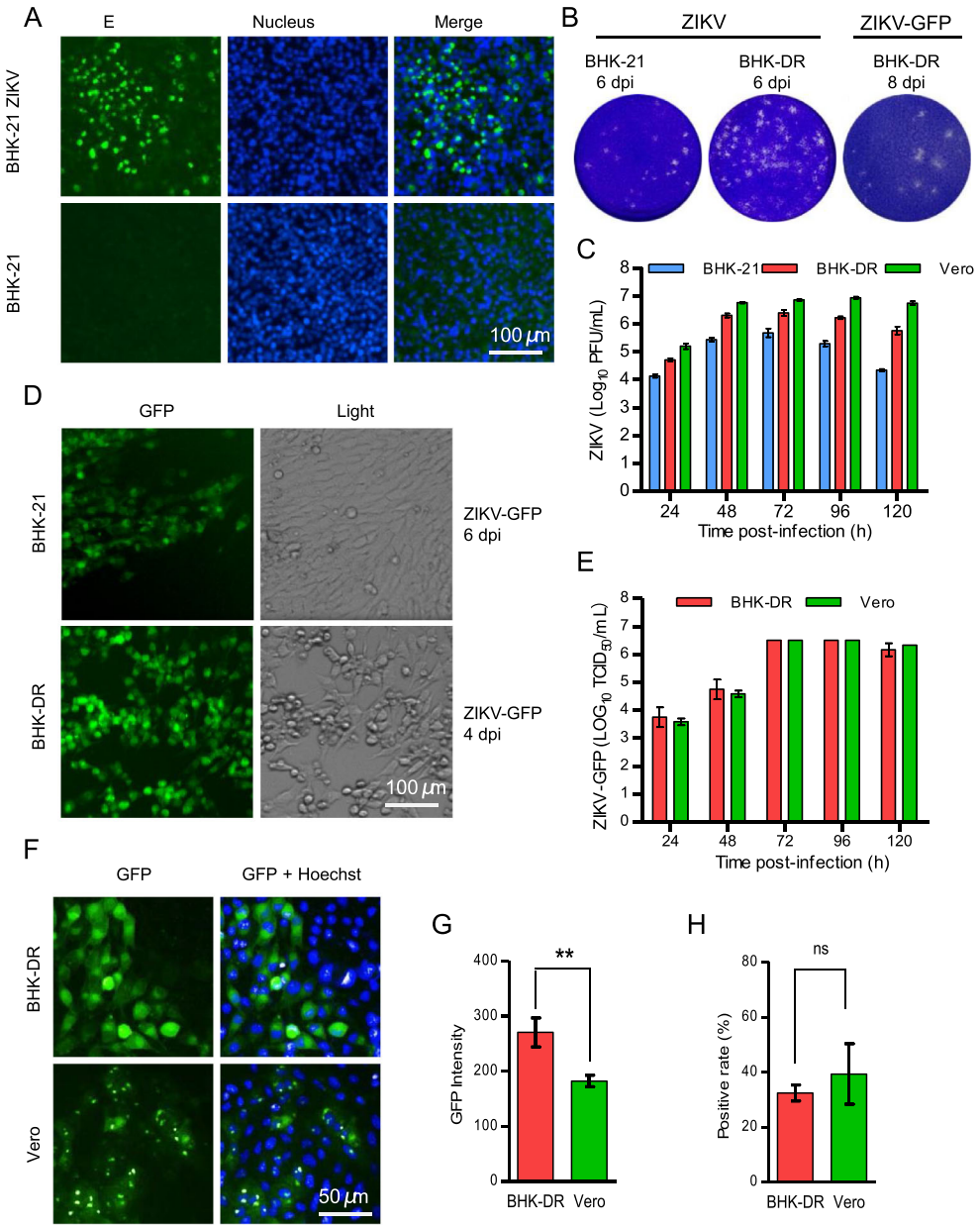

Fig. 2 Production and characterization of recombinant ZIKV and ZIKV-GFP reporter viruses. **A** Immunofluorescence analysis of recombinant ZIKV. The supernatants of transfected 293T cells were inoculated into BHK-21 cells. Forty-eight hours later, infected cells were fixed and probed with pan-flavivirus E proteinspecific MAb 4G2. Nuclei were stained with DAPI. **B** Representative images of plaque assays of BHK-21 and/or BHK-DR cells infected with ZIKV and ZIKV-GFP viruses and fixed and stained at the indicated days postinfection. **C** Replication kinetics of recombinant wild-type ZIKV in BHK-21, Vero and BHK-DR cells. Cells were infected at an MOI of 0.1. Supernatants were harvested at 24 hpi to 120 hpi and analyzed using a plaque form assay in BHK-21 cells. **D** ZIKV-GFP reporter virus infection in BHK-21 and BHK-DR cells. Cells infected with ZIKV-GFP at the indicated time were analyzed by fluorescence microscopy for GFP expression and by light microscopy for cytopathic effects. **E** Replication kinetics of recombinant ZIKV-GFP in Vero and BHK-DR cells. Cells were infected at an MOI of 0.1. Supernatants were harvest at 24 hpi to 120 hpi and analyzed using a TCID assay in BHK-DR cells by observation of fluorescent foci. **F** GFP fluorescence in Vero and BHK-DR cells infected with ZIKV-GFP. One representative experiment out of three is shown. At 48 hpi, cells were stained with DAPI and visualized using a high-content screening microplate imaging reader (Operetta; PerkinElmer). The GFP fluorescence intensity **G** and GFP-positive ratio **H** were analyzed using Acapella high-content imaging and analysis software. The results are the mean of three independent experiments performed in triplicate. Statistical significance was determined by the Student's *t*-test (** $P < 0.01$, ns $P > 0.05$).

cells (Fig. 2E). We further assessed the infectivity of ZIKV-GFP in BHK-DR and Vero cells with a high-content screening system. Unlike the dot-like fluorescence observed in Vero cells, GFP fluorescence was observed

throughout the cytoplasm of BHK-DR cells (Fig. 2F) and the cell outline was clearly identifiable. The GFP fluorescence intensity in infected BHK-DR cells was significantly higher than that in Vero cells (Fig. 2G), but the frequency of GFP-positive cells did not differ significantly between Vero and BHK-DR cells (Fig. 2H). These results indicate that the BHK-DR cell line was suitable for the propagation and visualization of the ZIKV-GFP reporter virus.

Recombinant Reporter Virus ZIKV-GFP can be Used for High-throughput Screening for ZIKV Inhibitors

To assess whether the recombinant ZIKV-GFP reporter virus and BHK-DR cell system could be applied to the high-throughput screening for inhibitors of ZIKV, a reported inhibitor of ZIKV, chloroquine (CQ) (Delvecchio *et al*. 2016; Li *et al*. 2017a), was tested for its ability to inhibit infection of BHK-DR cells by ZIKV-GFP. Treatment with CQ inhibited ZIKV-GFP replication in BHK-DR cells in a dose-dependent manner (Supplementary Fig. S2). The number of infected BHK-DR cells was clearly reduced by CQ at a concentration of 4 μmol/L (Supplementary Fig. S2A). This observation was confirmed by quantitatively analyzing the infection rate using Acapella high-content imaging and analysis. The relative infectivity of cells treated with CQ at 4 μmol/L or a higher dose was significantly lower than that of vehicle-treated cells (Supplementary Fig. S2C). The calculated IC_{50} value of CQ was 3.96 μmol/L, which was similar to previously published results with diverse screening systems (Li *et al*. 2017a).

The high-throughput system to screen ZIKV-GFP and BHK-DR cells was further evaluated using another reported flavivirus inhibitor, 6-azauridine (6-Az) (Lo *et al*. 2003; Adcock *et al*. 2017). Infection by ZIKV-GFP was inhibited by 6-Az at an IC_{50} of 7.16 μmol/L (Supplementary Fig. S2F), which was relatively consistent with the previously reported IC_{50} of 11 μmol/L against WNV (Lo *et al*. 2003) and an IC_{50} of 3.18 μmol/L against ZIKV strain MR766 (Adcock *et al*. 2017). A 6-Az concentration of 4 μmol/L significantly decreased the virus infectivity of treated cells ($P < 0.001$) compared with that of vehicle-treated cells (Supplementary Fig. S2G). These results demonstrate that the HTS assay with ZIKV-GFP and BHK-DR cells was effective and reliable.

Screening of A Selected Plant-sourced Compound Library for Inhibitors of ZIKV Infection

To discover novel anti-ZIKV compounds or to repurpose approved drugs, we screened a library of 974 selected plant-sourced compounds for anti-ZIKV activity using a high-throughput system schematically depicted in Fig. 3A. The first round of screening was conducted at a compound concentration of 10 μmol/L. At this concentration, most compounds showed little or no inhibition effect on ZIKV infection. The subset of compounds with a relative infection inhibition rate from –40% to 40% accounted for 76.4% of the total (Fig. 3B). Cell viabilities were evaluated by normalizing cell counts to those of vehicle-treated cells. In total, 95 compounds showed a relative infection inhibition rate of > 80%. Among these 95 compounds, 31 (indicated by red circles in Fig. 3C) were selected for further evaluation. The 31 hits included dihydroartemisinin (DHA), a well-known anti-malarial drug, and homoharringtonine (HHT), a drug used to treat myeloid leukemia (Chen *et al*. 2009, 2019).

Validation of Hit Drugs

In a primary screen, 31 compounds were selected for follow-up analysis based on the inhibition efficiency of ZIKV-GFP infection and the effect on cell counts. Each compound was used to pre-treat cells at concentrations of 0.1–100 μmol/L. As expected, most compounds displayed pronounced antiviral activity at a concentration of 10 μmol/L, which was consistent with the primary screen results. The selected 31 compounds included 19 with an $IC_{50} \leq 4$ μmol/L (Table 1) and the most potent of these were homoharringtonine (HHT), bruceine D (BD), dihydroartemisinin (DHA) and digitonin (DGT) (Fig. 3D). All these compounds inhibited viral infectivity in a dose-dependent manner (Fig. 4). The four compounds all possessed IC_{50} values less than 1 μmol/L. The virus infectivity of cells treated with HHT and BD at a concentration of 1 μmol/L was reduced by up to 90%; DHA and digitonin reduced virus infectivity by about 80%, without greatly affecting cell number, and showed CC_{50} values above 100 μmol/L (Fig. 4A). Cell number was significantly reduced by HHT and BD at a concentration of 100 μmol/L and the CC_{50} values were 50.66 and 25.66 μmol/L, respectively.

The inhibition efficiency of the four selected compounds was further confirmed using BHK-21 cells and the human cell line A549 infected with recombinant wild-type Zika virus (Fig. 5). As expected, most compounds displayed inhibitory activity: 0.5 μmol/L HHT inhibited the E protein level by over 90% in both BHK-21 and A549 cells (Fig. 5A, 5E). For BD, ZIKV E protein levels in both cell types were significantly decreased at concentrations of 0.5 μmol/L (Fig. 5B, 5F). Treatment with BHK-21 cells at a DGT concentration of 8 μmol/L and A549 cells with 2 μmol/L DGT significantly inhibited the expression of ZIKV E protein (Fig. 5C, 5G). DHA treatment efficiently

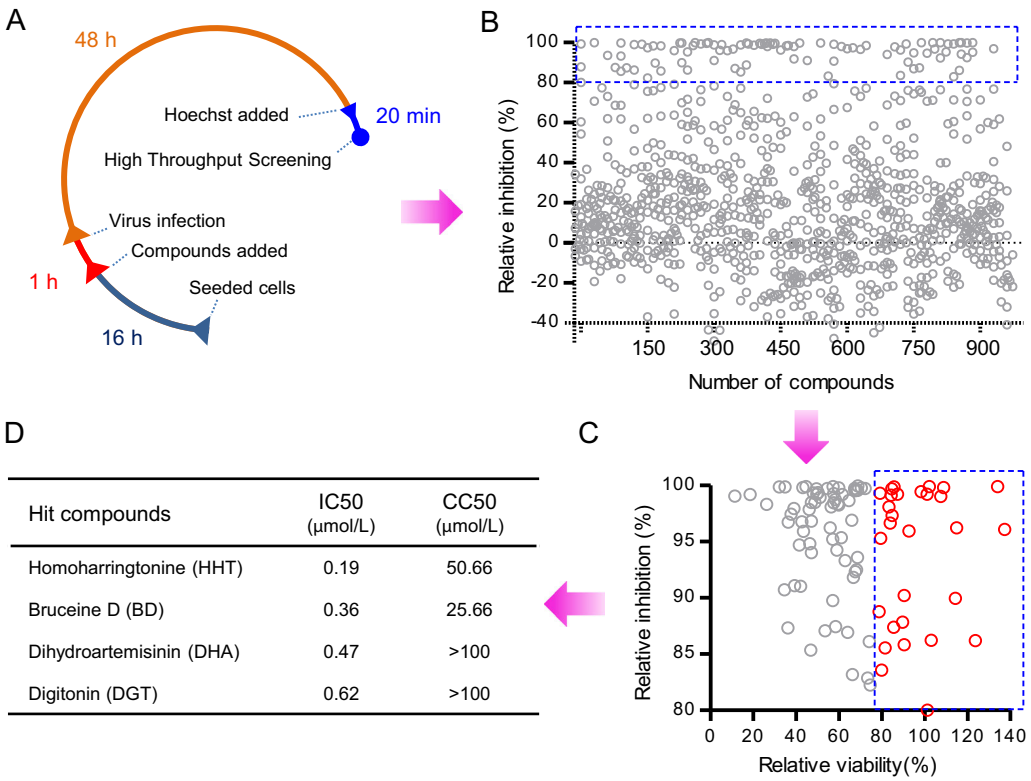

Fig. 3 High-throughput screening for inhibitors of ZIKV infection from a selected plant-sourced compound library. **A** High-throughput screening (HTS) assay timeline. BHK-DR cells were seeded in CellCarrier-96 microplates. After incubation for 16 h (usually overnight), cells were treated with compounds. One hour later, cells were infected with ZIKV-GFP for 48 h. The final concentration of compounds was 10 μmol/L. The final concentration of vehicle (DMSO) was 1%. Cell nuclei were stained with Hoechst for 20 min. The plates were scanned using a high-content-screening microplate imaging reader. **B** High-throughput screening of a library of 974 selected plant-sourced compounds. Each circle represents the percentage inhibition achieved with each compound at a concentration of 10 μmol/L. The circles within the blue box represent an inhibition > 80%. In total, 103 compounds causing a virus infection inhibition rate of > 80% were selected for further analysis of relative cell viability. **C** Out of 103 compounds from the primary selection, 31 compounds represented by red hollow circles within the blue-dotted square passed the criterion of relative cell viability > 80% at a concentration of 10 μmol/L. These compounds were selected for a confirmatory screen. **D** IC_{50} and CC_{50} of the top four selected compounds.

reduced the ZIKV E protein level in BHK-21 cells but only slightly inhibited that in A549 cells (Fig. 5D, 5H).

HHT, BD and DHA Inhibit ZIKV Infection at A Post-entry Stage, Whereas DGT Is Effective at A Pre-entry Stage

To investigate the underlying cellular mechanism of the hit compounds that inhibited ZIKV replication, time-of-addition experiments were performed (Fig. 6A). The HHT (Fig. 6B), BD (Fig. 6C) and DHA (Fig. 6D) compounds all inhibited ZIKV infection at the post-entry stage, but not at the pre-entry stage or during infection. However, DGT reduced ZIKV E protein expression at all stages, including virus pretreatment, cells pretreatment, during infection and at the post-entry stage of ZIKV (Fig. 6E). Digitonin is a natural plant detergent, which affects the membrane proteins of viruses or cells and might inhibit the binding of viruses or their entry into host cells. Therefore, DGT exhibits an inhibitory effect at the early stage of ZIKV infection. This hypothesis requires further testing.

Discussion

Reverse-genetic systems are powerful tools with which to study virus biology and pathogenesis. Using different strategies of reverse-genetic systems, the classical African lineage strain MR-766 (Gadea *et al*. 2016; Schwarz *et al*. 2016; Widman *et al*. 2017; Münster *et al*. 2018), Asian lineage strain FSS13025 (Shan *et al*. 2016; Yang *et al*. 2017) and recent outbreak epidemic strains (Tsetsarkin *et al*. 2016; Weger-Lucarelli *et al*. 2017; Widman *et al*. 2017; Deng *et al*. 2017) of ZIKV were generated. In this study, we generated a recombinant ZIKV of Brazil 2015 epidemic strain via a homologous recombination reverse-

Table 1 Evaluation of the primary HTS selected compounds.

Compounds	IC50 μmol/L	CC50 μmol/L
Homoharringtonine	0.19	50.66
Bruceine D	0.36	25.66
Cucurbitacin B	0.26	15.66
Dihydroartemisinin	0.47	> 100
Digitonin	0.62	> 100
Plumbagin	0.41	12.56
Schizandrin A	0.42	21.53
Dihydrochelerythrine	0.49	> 100
Betulonic acid	0.52	44.54
Artesunate	0.57	> 100
Sodium aescinate	0.69	> 100
Escin	0.76	> 100
Oleanonic acid	1.99	32.61
Cepharanthine	2.25	29.85
Corosolic acid	2.62	9.99
Bergamotine	2.98	23.76
Harringtonine	3.02	21.34
Schisanhenol	3.02	21.34
Fangchinoline	3.78	38.58
Fangchinoline	4.39	40.10
Dihydroactinidiolide	4.66	> 100
Schizandrin B	6.00	41.18
Tetrandrine	6.37	19.35
Liriope muscari baily saponins C	7.78	28.32
Ophiopogonin D	7.78	28.32
Saikosaponin A	9.22	27.72
Berbamine dihydrochloride	9.79	40.32
Daurisoline	10.13	29.28
Reserpine	10.20	33.33
Curcumin	11.23	> 100
Magnolol	31.37	> 100

After primary HTS, 31 compounds were selected for follow-up analysis. Each compound was used to pre-treat cells at concentrations of 0.1 μmol/L, 0.25 μmol/L, 0.5 μmol/L, 1 μmol/L, 2 μmol/L, 4 μmol/L, 10 μmol/L and 100 μmol/L. The vehicle was used as negative control. After 48 h of infection, cell nuclei were stained with Hoechst. Then the plates were scanned by using a high-content-screening microplate imaging reader. Fifty nine fields per well were scanned using 20× objective and analysed for percentage of infection and cell number. The infection positive cell rates and total cell counts were all normalized to that of vehicle control wells.

genetic strategy, which involved cloning the ZIKV genome in two steps. Firstly, one-quarter of the genome that contains the 5′UTR, structural protein-coding sequences and the partial NS1-coding sequence was cloned into a plasmid under transcriptional control of the CMV promoter. The remaining three-quarters of the genome was constructed as a replicon plasmid. This reverse-genetic system overcame the difficulty of constructing a stable full-length flavivirus cDNA clone and furthermore, it is convenient to directly transfect cells with PCR products and plasmid DNA without *in vitro* transcription. Our results and previous reports have shown that this strategy is also highly efficient (Aubry *et al*. 2014; Atieh *et al*. 2016). In addition, the method provides a flexible strategy for constructing reporter viruses that express different foreign genes (Gadea *et al*. 2016), because only the plasmid containing the first quarter of the viral genome and the foreign gene needs to be reconstituted.

The use of a reporter virus can visualize the infection and replication of viruses in cells and is a powerful tool for studying viral replication mechanisms and to screen for antiviral drugs. However, to date, all reporter Zika viruses, including the expression of a luciferase reporter virus (Shan *et al*. 2016; Münster *et al*. 2018) or GFP reporter virus (Gadea *et al*. 2016) were unstable and their replication in cells was attenuated. These shortcomings limit the use of reporter viruses in the high-throughput screening of drugs and the mechanism of attenuated replication of reporter viruses in cells remains unknown. We observed that the replication of ZIKV-GFP in cells is slower than that of wild-type ZIKV, and the amount of green fluorescent foci increased slowly (Supplementary Fig. S1). These observations suggest that ZIKV-GFP mainly spreads via cell-to-cell contact infection, and that cell-free infection is weak. We hypothesized that increasing the cell-free infection of ZIKV-GFP might promote the replication efficiency of ZIKV-GFP in cells. Therefore, to increase viral infectivity in this study, we established a DC-SIGNR stably expressed cell line, BHK-DR, to promote viral replication. Because DC-SIGNR is a putative receptor of ZIKV and other flaviviruses (Navarro-Sanchez *et al*. 2003; Davis *et al*. 2006; Fernandez-Garcia *et al*. 2009; Shimojima *et al*. 2014; Hamel *et al*. 2015), its expression was expected to improve the replication efficiency of ZIKV-GFP and indeed, this was the case. This increase in replication efficiency potentially reduced the genetic stress of ZIKV-GFP. The reporter virus ZIKV-GFP remained stable in BHK-DR cells for at least five passages (data not shown).

Another potential reason for the observed increase in the replication efficiency and stability of the reporter virus is the number of amino acid residues of the C protein upstream of the foreign gene. We retained 38 amino acid residues of the C protein at the translation initiation. In fact, we also compared the effect of the retained length of C protein on the rescue of virus in this study. When only 28 residues were retained, the rescue efficiency of the reporter virus was lowest, few green fluorescent foci were observed and the reporter virus could be rescued occasionally. When 33 and 38 amino acid residues were retained, the virus

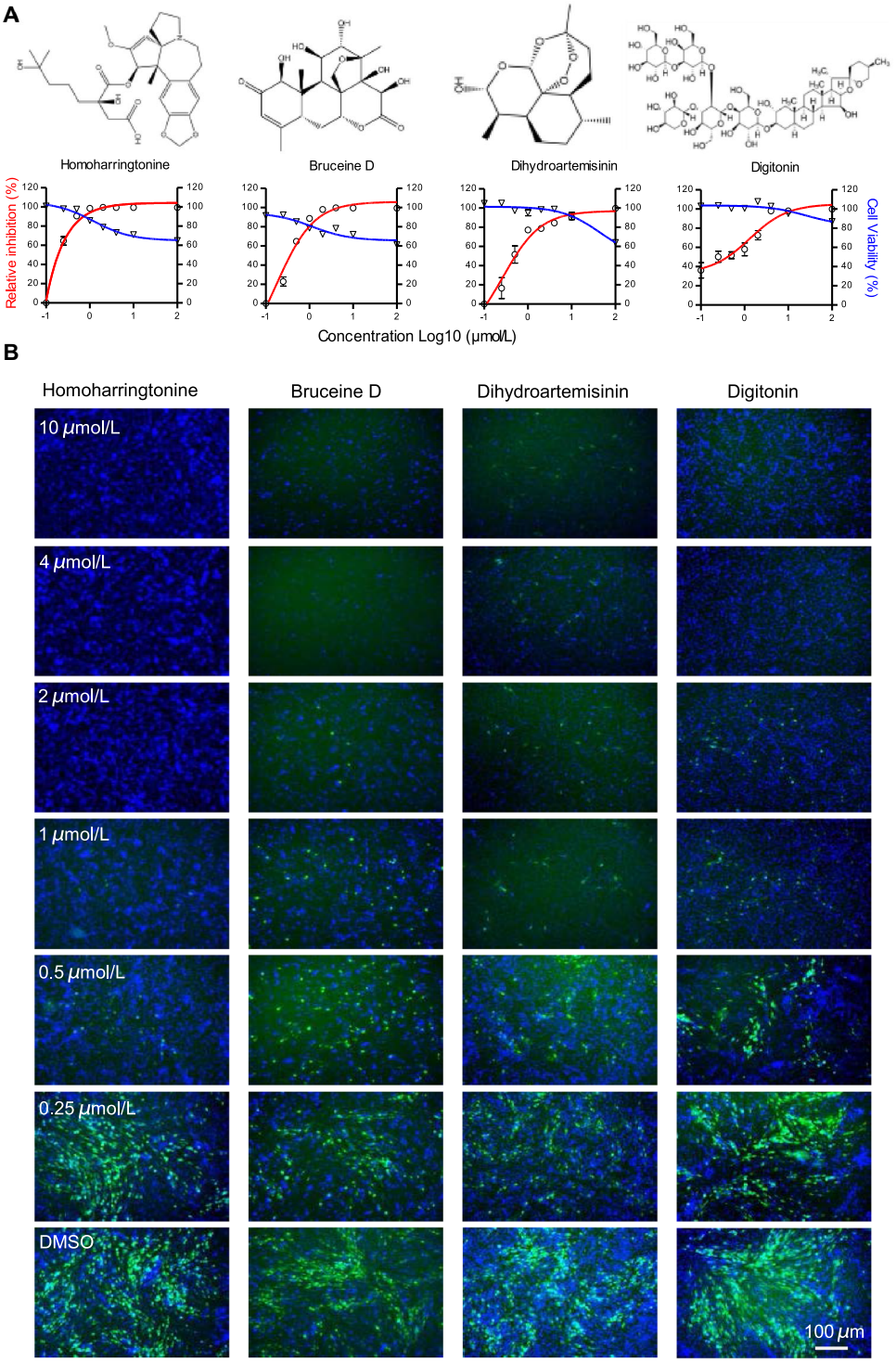

Fig. 4 Validation of the antiviral effects of the hit compounds. **A** Top: The chemical structures of the hit compounds homoharringtonine (HHT), dihydroartemisinin (DHA), digitonin (DGT) and bruceine D (BD). Bottom: Dose–response curves showing the effect of compound treatment on virus infection inhibition (red) and cell viability (blue) in BHK-DR cells infected with ZIKV-GFP. Values represent the means ± SD from two independent experiments performed in triplicate. The data are normalized to those of DMSO-treated cells. **B** Representative fluorescence images of BHK-DR cells treated with varying concentrations of hit compounds. BHK-DR cells were treated with the indicated compounds at the indicated final concentrations and were infected after 1 h with reporter virus at an MOI of 0.1. Cells treated with DMSO at a final concentration of 1% were used as a vehicle control. At 48 hpi, cell nuclei were stained with Hoechst and cell plates were scanned using a high-content-screening microplate imaging reader.

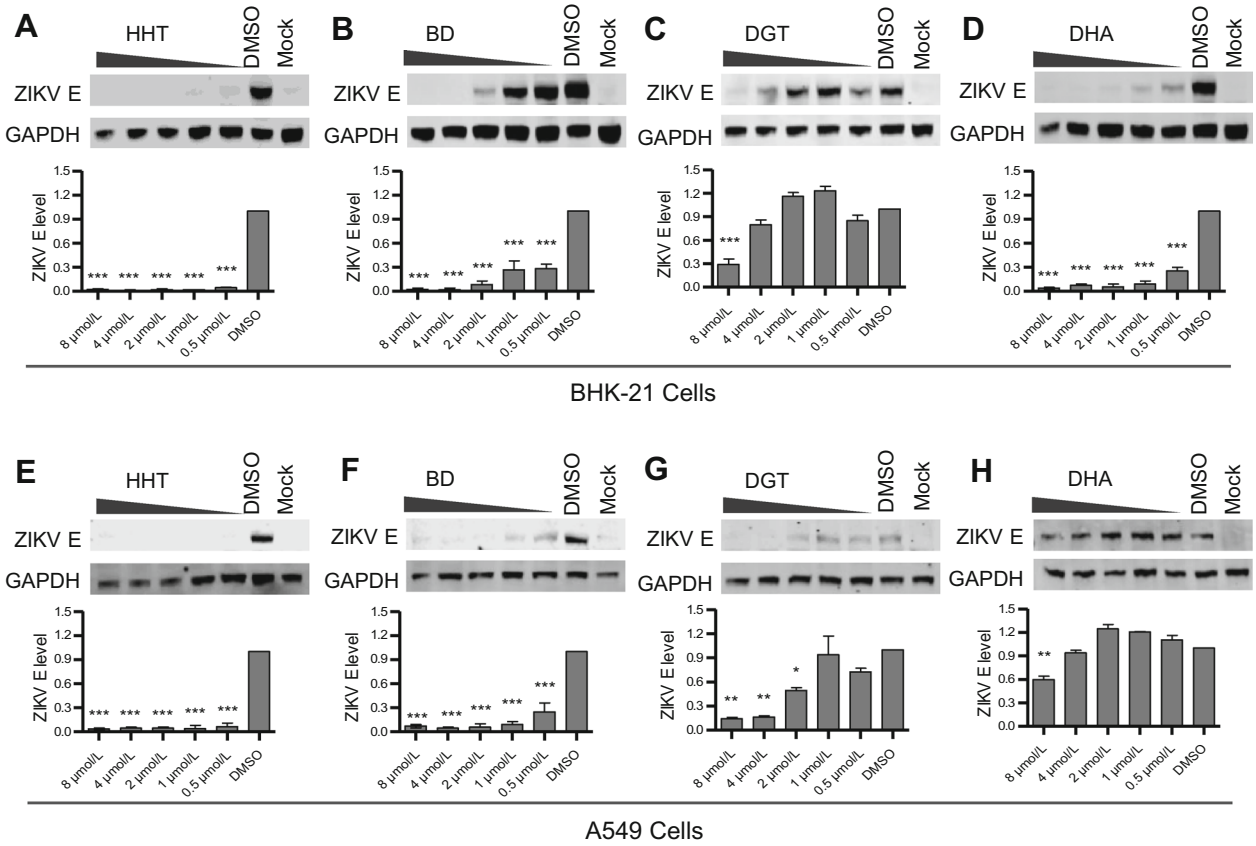

Fig. 5 Confirmation of the inhibitory effect of selected compounds on ZIKV in BHK-21 and A549 cells. Each compound was used to pretreat indicated cells at concentrations of 8 μmol/L, 4 μmol/L, 2 μmol/L, 1 μmol/L and 0.5 μmol/L for 1 h prior to infection with wild-type ZIKV at an MOI of 0.01. Vehicle-treated cells and uninfected cells were used as controls. At 48 hpi, the cell lysates were analyzed by immunoblotting for ZIKV E protein expression, and the virus titer in the culture supernatants was measured on BHK-21 cells. BHK-21 cells treated with **A** HHT, **B** BD, **C** DGT and **D** DHA. Top: Representative western blot images. Bottom: Quantification of E protein band intensities relative to those for GAPDH. Data were normalized to those of DMSO-treatment cells. The data were pooled from two independent experiments. Values represent the mean ± SD. Statistical significances were determined by one-way ANOVA, compared to DMSO-treated cells (***$P < 0.001$). A549 cells treated with **E** HHT, **F** BD, **G** DGT and **H** DHA. Top: Representative western blot images. Bottom: Quantification of E protein band intensities relative to those for GAPDH. Data were normalized to those of DMSO-treatment cells. The data were pooled from two independent experiments. Values represent the mean ± SD. Statistical significances were determined by one-way ANOVA compared to DMSO-treated cells (*$P < 0.05$; **$P < 0.01$; ***$P < 0.001$).

could be rescued almost every time, and the retention of 38 residues led to the best replication efficiency (Supplementary Fig. S3).

To counter ZIKV-associated disease, efforts to develop effective anti-ZIKV drugs have increased worldwide and different platforms or systems have been established to screen for inhibitors of ZIKV. In addition to standard IFA and virus titration methods (Barrows *et al*. 2016), an assay with *Renilla* luciferase (Rluc) expressing the ZIKV replicon (Xie *et al*. 2016), the caspase-3 activity assay (Xu *et al*. 2016) and the *Renilla* luciferase reporter virus assay (Shan *et al*. 2016; Münster *et al*. 2018) have been developed to screen for anti-ZIKV drugs. Here, we have established a high-throughput screening platform for anti-ZIKV drugs using the BHK-DR cell line and the ZIKV-GFP reporter virus. In this system, the reporter virus is highly stable and has a high replication efficiency. Compared with the luciferase-expressing reporter virus screening system, our system does not necessitate the exchange of culture media or substrate addition and the results can be directly visualized and analyzed by live-cell imaging scanning.

Medicinal plants are a valuable source of therapeutic agents. Many of today's drugs originate from natural plant products or their derivatives, such as the anti-cancer agent paclitaxel and its derivatives (Kingston 2011; Cragg and Newman 2013) and the anti-malarial agent artemisinin (Atanasov *et al*. 2015). Out of the drugs considered to be basic and essential by the WHO, 11% originate exclusively from flowering plants (Veeresham 2012). Natural products remain a rich source of new antiviral leads, which might have broad-spectrum antiviral activities with novel mechanisms of action or improved resistance profiles. Using

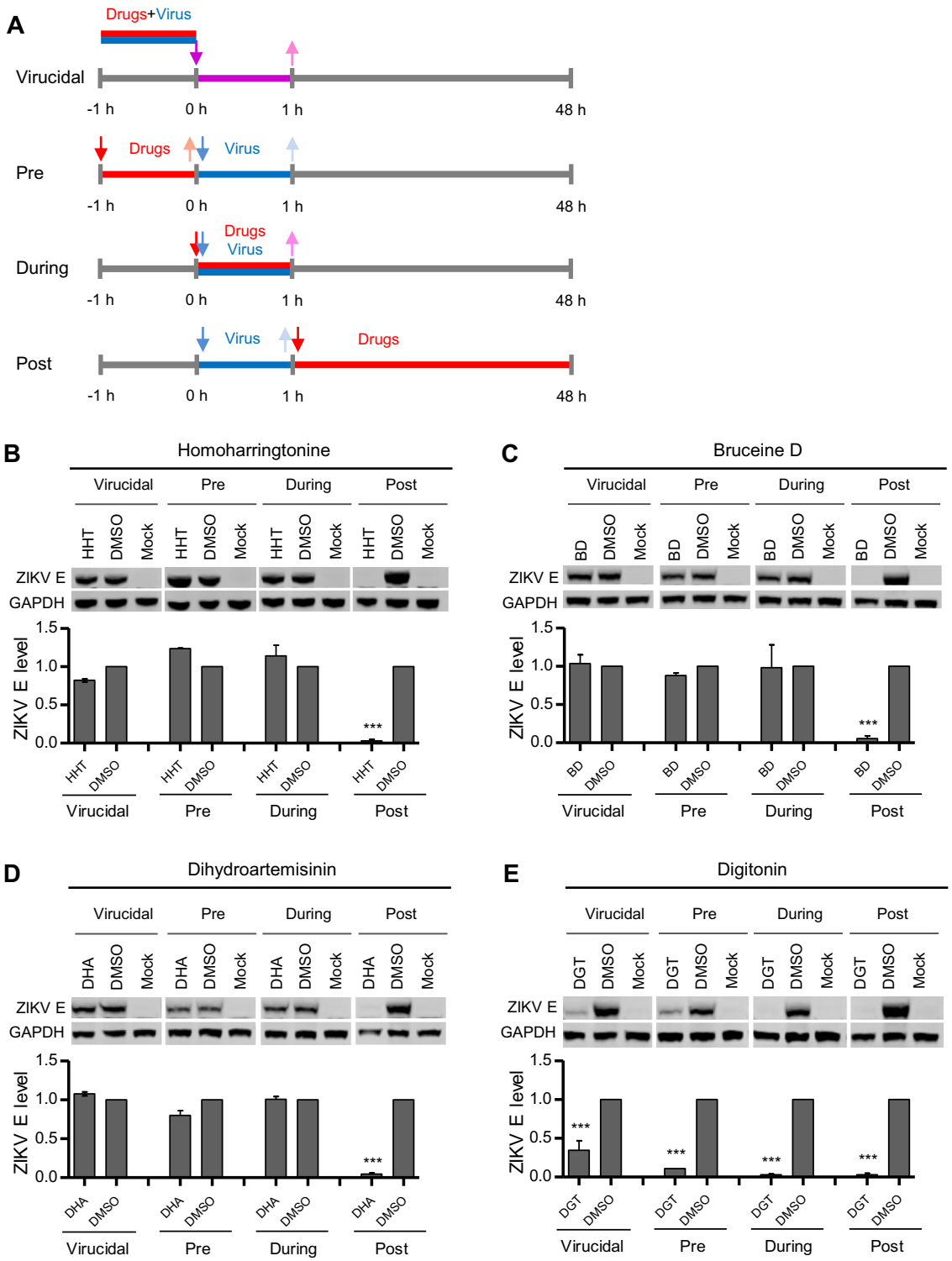

Fig. 6 Time-of-addition analysis of the antiviral activity of the hit compounds. **A** Schematic illustration of the time-of-addition experiment. **B**, **C**, **D** and **E** BHK-21 cells were infected with ZIKV at an MOI of 0.01 for 1 h (0 to 1 h). Either 1 μmol/L HHT (**B**), 4 μmol/L BD (**C**), 4 μmol/L DHA (**D**), or 8 μmol/L DGT (**E**) were introduced at different time points of ZIKV infection, designated virucidal, pretreatment (pre), during treatment (during), or posttreatment (post). The inhibitory effect of the compounds in each group was determined by immunoblotting for E protein expression. Top: Representative western blot images. Bottom: Quantification of E protein band intensities relative to those for GAPDH. Data were normalized to those of DMSO-treatment cells. The data were pooled from two independent experiments. Values represent the mean ± SD. Statistical significances were determined by one-way ANOVA compared to DMSO-treated cells (***$P < 0.001$).

GFP expression as a read-out of Zika virus infectivity, we screened a selected plant-sourced compound library containing 974 compounds from 277 plant species. Homoharringtonine and bruceine D exhibited broad-spectrum inhibitory activity against ZIKV, Japanese encephalitis virus (JEV) and West Nile virus (WNV). Homoharringtonine is a natural product first discovered in the evergreen tree *Cephalotaxus harringtonia*, native to southern China. It has been used in China to treat chronic myeloid leukemia (CML), acute myeloid leukemia (AML) and myelodysplastic syndrome (MDS) for the past 40 years (Jin *et al*. 2006; Chen *et al*. 2019). Omacetaxine, a semisynthetic form of HHT, was approved by FDA in 2012 for the treatment of CML (Lü and Wang 2014). Besides the broad spectrum anti-flavivirus activities described here, HHT shows broad-spectrum inhibition of viruses from six families, including DNA and RNA viruses (Dong *et al*. 2018). Homoharringtonine has the potential to be repurposed as a broad-spectrum antiviral drug. Although the FDA lists it as a pregnancy Class D drug, it can be used in other infected individuals such as Guillain-Barré syndrome patients. Dihydroartemisinin is another FDA-approved antimalarial drug; however, its inhibitory effect against ZIKV in A549 cells was not as good as that in BHK21 cells and whether DHA can be used as an anti-ZIKV drug requires further evaluation. Bruceine D is a newly screened anti-ZIKV compound in this study. Its antiviral mechanism and its potential use as a drug remain to be further evaluated. Digitonin has inhibitory activity in the early stages of viral infection and is a non-ionic detergent, which also suggests that one positive method to prevent viral infections is via enhancing personal and environmental hygiene.

Most importantly, the data presented here describe an efficient and convenient high-throughput screening assay for ZIKV inhibitors, in addition to providing an additional approach towards anti-ZIKV drug development.

Acknowledgements This work was partially supported by the National Key R&D Program of China (grant 2018YFC1200602 and 2016YFD0500403 to RHH).

Author contributions RHH and ZGB designed the study. RHH, JWZ, HW, LM, JL performed the experiments. RHH and JWZ analyzed the data and drafted the manuscript. RHH and ZGB finalized the manuscript. All authors read and approved the final manuscript.

Compliance with Ethical standards

Conflict of interest The authors declare that they have no conflict of interest.

Animal and Human Rights Statement This article does not contain any studies with human or animal subjects peformed by any of the authors.

References

Adcock RS, Chu Y-K, Golden JE, Chung D-H (2017) Evaluation of anti-Zika virus activities of broad-spectrum antivirals and NIH clinical collection compounds using a cell-based, high-throughput screen assay. Antivir Res 138:47–56

Aoki-Utsubo C, Chen M, Hotta H (2018) Time-of-addition and temperature-shift assays to determine particular step(s) in the viral life cycle that is blocked by antiviral substance(s). BIO-Protoc 8(9):e2830

Atanasov AG, Waltenberger B, Pferschy-Wenzig EM, Linder T, Wawrosch C, Uhrin P, Temml V, Wang L, Schwaiger S, Heiss EH, Rollinger JM, Schuster D, Breuss JM, Bochkov V, Mihovilovic MD, Kopp B, Bauer R, Dirsch VM, Stuppner H (2015) Discovery and resupply of pharmacologically active plant-derived natural products: a review. Biotechnol Adv 33:1582–1614

Atieh T, Baronti C, de Lamballerie X, Nougairède A (2016) Simple reverse genetics systems for Asian and African Zika viruses. Sci Rep 6:39384

Aubry F, Nougairede A, de Fabritus L, Querat G, Gould EA, de Lamballerie X (2014) Single-stranded positive-sense RNA viruses generated in days using infectious subgenomic amplicons. J Gen Virol 95:2462–2467

Barrows NJ, Campos RK, Powell ST, Prasanth KR, Schott-Lerner G, Soto-Acosta R, Galarza-Munoz G, McGrath EL, Urrabaz-Garza R, Gao J, Wu P, Menon R, Saade G, Fernandez-Salas I, Rossi SL, Vasilakis N, Routh A, Bradrick SS, Garcia-Blanco MA (2016) A Screen of FDA-approved drugs for inhibitors of Zika virus infection. Cell Host Microbe 20:259–270

Chen Y, Hu Y, Michaels S, Segal D, Brown D, Li S (2009) Inhibitory effects of omacetaxine on leukemic stem cells and BCR-ABL-induced chronic myeloid leukemia and acute lymphoblastic leukemia in mice. Leukemia 23:1446–1454

Chen M, Aoki-Utsubo C, Kameoka M, Deng L, Terada Y, Kamitani W, Sato K, Koyanagi Y, Hijikata M, Shindo K, Noda T, Kohara M, Hotta H (2017) Broad-spectrum antiviral agents: secreted phospholipase A2 targets viral envelope lipid bilayers derived from the endoplasmic reticulum membrane. Sci Rep 7:15931

Chen X, Tang Y, Chen J, Chen R, Gu L, Xue H, Pan C, Tang J, Shen S (2019) Homoharringtonine is a safe and effective substitute for anthracyclines in children younger than 2 years old with acute myeloid leukemia. Front Med 13:378–387

Chitti SV, Prasad AK, Saxena SK (2016) Emerging Zika virus disease: a public health emergency of global concern. VirusDisease 27:211–214

Cragg GM, Newman DJ (2013) Natural products: a continuing source of novel drug leads. Biochim Biophys Acta 1830:3670–3695

Davis CW, Nguyen H-Y, Hanna SL, Sanchez MD, Doms RW, Pierson TC (2006) West Nile virus discriminates between DC-SIGN and DC-SIGNR for cellular attachment and infection. J Virol 80:1290–1301

Delvecchio R, Higa L, Pezzuto P, Valadão A, Garcez P, Monteiro F, Loiola E, Dias A, Silva F, Aliota M, Caine E, Osorio J, Bellio M, O'Connor D, Rehen S, de Aguiar R, Savarino A, Campanati L, Tanuri A (2016) Chloroquine, an endocytosis blocking agent, inhibits Zika virus infection in different cell models. Viruses 8:322

Deng C-L, Zhang Q-Y, Chen D-D, Liu S-Q, Qin C-F, Zhang B, Ye H-Q (2017) Recovery of the Zika virus through an *in vitro* ligation approach. J Gen Virol 98:1739–1743

Dick GWA, Kitchen SF, Haddow AJ (1952) Zika virus (I). Isolations and serological specificity. Trans R Soc Trop Med Hyg 46:509–520

Dong H-J, Wang Z-H, Meng W, Li C-C, Hu Y-X, Zhou L, Wang X-J (2018) The natural compound homoharringtonine presents broad antiviral activity *in vitro* and *in vivo*. Viruses 10:601

Fernandez-Garcia M-D, Mazzon M, Jacobs M, Amara A (2009) Pathogenesis of Flavivirus infections: using and abusing the host cell. Cell Host Microbe 5:318–328

França GVA, Schuler-Faccini L, Oliveira WK, Henriques CMP, Carmo EH, Pedi VD, Nunes ML, Castro MC, Serruya S, Silveira MF, Barros FC, Victora CG (2016) Congenital Zika virus syndrome in Brazil: a case series of the first 1501 livebirths with complete investigation. Lancet 388:891–897

Gadea G, Bos S, Krejbich-Trotot P, Clain E, Viranaicken W, El-Kalamouni C, Mavingui P, Despres P (2016) A robust method for the rapid generation of recombinant Zika virus expressing the GFP reporter gene. Virology 497:157–162

Gulland A (2016) Zika virus is a global public health emergency, declares WHO. BMJ i657

Hamel R, Dejarnac O, Wichit S, Ekchariyawat P, Neyret A, Luplertlop N, Perera-Lecoin M, Surasombatpattana P, Talignani L, Thomas F, Cao-Lormeau V-M, Choumet V, Briant L, Desprès P, Amara A, Yssel H, Missé D (2015) Biology of Zika virus infection in human skin cells. J Virol 89:8880–8896

Hua R-H, Huo H, Li Y-N, Xue Y, Wang X-L, Guo L-P, Zhou B, Song Y, Bu Z-G (2014) Generation and efficacy evaluation of recombinant classical Swine fever virus E2 glycoprotein expressed in stable transgenic mammalian cell line. PLoS ONE 9:e106891

Hua RH, Li YN, Chen ZS, Liu LK, Huo H, Wang XL, Guo LP, Shen N, Wang JF, Bu ZG (2014) Generation and characterization of a new mammalian cell line continuously expressing virus-like particles of Japanese encephalitis virus for a subunit vaccine candidate. BMC Biotechnol 14:62

Jin J, Jiang DZ, Mai WY, Meng HT, Qian WB, Tong HY, Huang J, Mao LP, Tong Y, Wang L, Chen ZM, Xu WL (2006) Homoharringtonine in combination with cytarabine and aclarubicin resulted in high complete remission rate after the first induction therapy in patients with de novo acute myeloid leukemia. Leukemia 20:1361–1367

Kingston DGI (2011) Modern natural products drug discovery and its relevance to biodiversity conservation. J Nat Prod 74:496–511

Kobayashi S, Yoshii K, Hirano M, Muto M, Kariwa H (2017) A novel reverse genetics system for production of infectious West Nile virus using homologous recombination in mammalian cells. J Virol Methods 240:14–20

Li C, Zhu X, Ji X, Quanquin N, Deng YQ, Tian M, Aliyari R, Zuo X, Yuan L, Afridi SK, Li XF, Jung JU, Nielsen-Saines K, Qin FX, Qin CF, Xu Z, Cheng G (2017) Chloroquine, a FDA-approved drug, prevents Zika virus infection and its associated congenital microcephaly in mice. EBioMedicine 24:189–194

Li W, Ma L, Guo L-P, Wang X-L, Zhang J-W, Bu Z-G, Hua R-H (2017) West Nile virus infectious replicon particles generated using a packaging-restricted cell line is a safe reporter system. Sci Rep 7:3286

Lo MK, Tilgner M, Shi P-Y (2003) Potential high-throughput assay for screening inhibitors of West Nile virus replication. J Virol 77:12901–12906

Lü S, Wang J (2014) Homoharringtonine and omacetaxine for myeloid hematological malignancies. J Hematol OncolJ Hematol Oncol 7:2

Münster M, Płaszczyca A, Cortese M, Neufeldt C, Goellner S, Long G, Bartenschlager R (2018) A reverse genetics system for Zika virus based on a simple molecular cloning strategy. Viruses 10:368

Navarro-Sanchez E, Altmeyer R, Amara A, Schwartz O, Fieschi F, Virelizier J-L, Arenzana-Seisdedos F, Desprès P (2003) Dendritic-cell-specific ICAM3-grabbing non-integrin is essential for the productive infection of human dendritic cells by mosquito-cell-derived dengue viruses. EMBO Rep 4:723–728

Petersen EE, Staples JE, Meaney-Delman D, Fischer M, Ellington SR, Callaghan WM, Jamieson DJ (2016) Interim guidelines for pregnant women during a Zika virus outbreak—United States, 2016. MMWR Morb Mortal Wkly Rep 65:30–33

Pu SY, Wu RH, Yang CC, Jao TM, Tsai MH, Wang JC, Lin HM, Chao YS, Yueh A (2011) Successful propagation of Flavivirus infectious cDNAs by a novel method to reduce the cryptic bacterial promoter activity of virus genomes. J Virol 85:2927–2941

Schwarz MC, Sourisseau M, Espino MM, Gray ES, Chambers MT, Tortorella D, Evans MJ (2016) Rescue of the 1947 Zika virus prototype strain with a cytomegalovirus promoter-driven cDNA clone. mSphere 1

Shan C, Xie X, Muruato Antonio E, Rossi Shannan L, Roundy Christopher M, Azar Sasha R, Yang Y, Tesh Robert B, Bourne N, Barrett Alan D, Vasilakis N, Weaver Scott C, Shi P-Y (2016) An infectious cDNA clone of Zika virus to study viral virulence, mosquito transmission, and antiviral inhibitors. Cell Host Microbe 19:891–900

Shimojima M, Takenouchi A, Shimoda H, Kimura N, Maeda K (2014) Distinct usage of three C-type lectins by Japanese encephalitis virus: DC-SIGN, DC-SIGNR, and LSECtin. Adv Virol 159:2023–2031

Tsetsarkin KA, Kenney H, Chen R, Liu G, Manukyan H, Whitehead SS, Laassri M, Chumakov K, Pletnev AG (2016) A full-length infectious cDNA clone of Zika virus from the 2015 epidemic in Brazil as a genetic platform for studies of virus-host interactions and vaccine development. mBio 7

Veeresham C (2012) Natural products derived from plants as a source of drugs. J Adv Pharm Technol Res 3:200

Weger-Lucarelli J, Duggal NK, Bullard-Feibelman K, Veselinovic M, Romo H, Nguyen C, Ruckert C, Brault AC, Bowen RA, Stenglein M, Geiss BJ, Ebel GD (2017) Development and characterization of recombinant virus generated from a new world Zika virus infectious clone. J Virol 91

Widman DG, Young E, Yount BL, Plante KS, Gallichotte EN, Carbaugh DL, Peck KM, Plante J, Swanstrom J, Heise MT, Lazear HM, Baric RS (2017) A Reverse genetics platform that spans the Zika virus family tree. mBio 8

Xie X, Zou J, Shan C, Yang Y, Kum DB, Dallmeier K, Neyts J, Shi PY (2016) Zika virus replicons for drug discovery. EBioMedicine 12:156–160

Xu M, Lee EM, Wen Z, Cheng Y, Huang W-K, Qian X, Tcw J, Kouznetsova J, Ogden SC, Hammack C, Jacob F, Nguyen HN, Itkin M, Hanna C, Shinn P, Allen C, Michael SG, Simeonov A, Huang W, Christian KM, Goate A, Brennand KJ, Huang R, Xia M, Ming G-l, Zheng W, Song H, Tang H (2016) Identification of small-molecule inhibitors of Zika virus infection and induced neural cell death via a drug repurposing screen. Nat Med 22:1101–1107

Yang Y, Shan C, Zou J, Muruato AE, Bruno DN, de Almeida Medeiros Daniele B, Vasconcelos PFC, Rossi SL, Weaver SC, Xie X, Shi P-Y, (2017) A cDNA clone-launched platform for high-yield production of inactivated Zika vaccine. EBioMedicine 17:145–156

Zheng X, Tong W, Liu F, Liang C, Gao F, Li G, Tong G, Zheng H (2016) Genetic instability of Japanese encephalitis virus cDNA clones propagated in Escherichia coli. Virus Genes 52:195–203

Publisher's Note

Springer Nature remains neutral with regard to jurisdictional claims in published maps and institutional affiliations.